Colloid Polym Sci (2007) 285:1741–1747
DOI 10.1007/s00396-007-1761-2

SHORT COMMUNICATION

Viscoelasticity and mass transfer in phenol–CTAB aqueous systems

Dharmesh Varade · Carlos Rodríguez-Abreu · José Gregorio Delgado · Kenji Aramaki

Received: 13 May 2007 / Revised: 5 July 2007 / Accepted: 10 August 2007 / Published online: 28 September 2007

Abstract The rheological and mass transport properties of phenol in micellar solutions of hexadecyltrimethylammonium bromide (CTAB) were studied by rheometry and spectrophotometry. The presence of phenol located between headgroups of the CTAB diminishes the repulsive forces between the cationic groups and induces a sharp increase in viscosity that is attributed to the one-dimensional micellar growth favoring the formation of worm-like micelles. It is found that the mass transfer of phenol between two immiscible phases is significantly retarded by the presence of CTAB. The transfer is particularly slow when the diffusion takes place from a surfactant solution phase to an organic phase. This behavior is attributed to the phenol–surfactant interaction that leads to micellar growth and viscoelastic behavior. However, at elevated temperature, viscosity decreases and mass transfer increases. This particular rheological behavior offers the possibility of regulating the mass transfer, which might be interesting for applications.

D. Varade · K. Aramaki (✉)
Graduate School of Environment and Information Sciences,
Yokohama National University,
Tokiwadai 79-7, Hodogaya-ku,
Yokohama 240-8501, Japan
e-mail: aramakik@ynu.ac.jp

C. Rodríguez-Abreu
Institut d`Investigacions Químiques i Ambientals
de Barcelona (IIQAB/CSIC),
Jordi Girona, 18-26,
08034 Barcelona, Spain

J. G. Delgado
Escuela de Ingeniería Química, Universidad de Los Andes,
Mérida 5101, Venezuela

Keywords Rheometry · Worm-like · Viscoelasticity · Spectrophotometry · Mass transfer

Introduction

The formation and properties of worm-like micelles in surfactant systems have drawn considerable interest in both basic research and practical applications [1, 2]. It is well known that long chain cationic surfactants like hexadecyltrimethylammonium bromide (CTAB) can self assemble into long, flexible worm-like micelles as a consequence of the reduction of the repulsion between surfactant headgroups, which can be induced by adding salts, strongly binding counterions or cosurfactants [3–12]. The entanglement of these micelles into a transient network imparts viscoelastic properties to the solution [13]. On the other hand, there are many reports on the solubilization of different compounds, which often leads to changes in micellar structure [14–20]. The amount of solubilizate, its location within the micelle, and its effect on micellar size depend significantly on the nature of the solubilizate and its interaction with the surfactant [21].

Solubilization phenomena have practical implications in, for example, micellar-enhanced ultrafiltration (MEUF) of aromatic contaminants, in which the retentate is a highly concentrated stream-containing surfactant micelles solubilizing the contaminant [22]. Additionally, the incorporation of phenol and aromatic amine monomers into micelles creates confined environments for the chemical or enzymatic synthesis of novel polyphenolics and polyaromatic amines [23–25]. Although it is known that solutions of cationic surfactants form gels in the presence of aromatic compounds [26–29], still, there is a need to correlate the change in rheological properties with the micellar structure

and diffusion properties of the additive. Surprisingly, there are very few studies on the diffusion of additive into or from worm–micellar solutions, which can be potential candidates for drug delivery systems.

In this context, we have investigated the rheology and mass transfer of phenol in the presence of the cationic surfactant CTAB. First, we describe the rheological behavior of phenol+CTAB aqueous systems. Then, we present results on the mass transfer of the phenol towards aqueous and organic phases, trying to find a correlation with the rheological behavior of the system.

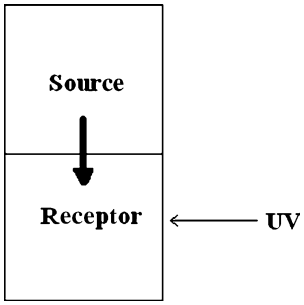

Scheme 1 Arrangement of the immiscible phases in the cuvette for the contacting experiment. The *thick arrow* indicates the direction of phenol transfer

Experimental section

Materials

CTAB purity >99% was purchased from Fluka. Phenol (purity >98%) and tetrachloroethylene (purity >97%) were obtained from Wako Pure Chemical Industries, Japan. AR grade Octanol was from TCI, Japan. All the chemicals were used as received. Millipore-filtered water was used for the preparation of all the samples.

Methods

Rheological measurements Samples for the rheological measurements were homogenized and kept in water bath at specified temperature for at least 24 h to ensure equilibration before performing measurements. The rheological measurements were performed in a stress-controlled rheometer, AR-G2 (TA Instrument) using cone-plate geometry with the plate temperature controlled by a peltier unit. A sample cover provided with the instrument was used to minimize the change in sample composition by evaporation during the measurement. Frequency sweep measurements were performed in the linear viscoelastic regime of the samples, as determined previously by dynamic strain sweep measurements. The zero-shear viscosity of the samples was determined from the steady shear-rate measurement of samples by extrapolating the viscosity–shear rate curve to zero shear rate. Both steady and dynamic rheological experiments were performed at different temperatures.

UV spectrometry UV spectra were collected using an Agilent 8543 with a temperature controller (Agilent 89090A). For measuring the mass transfer, a contacting method proposed by Williams et al. [30] was used, with an arrangement shown in Scheme 1. A known volume of 0.15 M CTAB (in one set) or water (in other), which is transparent in the UV region, was introduced in a spectrophotometer cuvette (quartz, 1-mm path length) using a micropipet. This phase is designated as the receptor. Next, a 10 wt% phenol solution in octanol was carefully placed on top of the lower solution with the tip very close to the wall and near the liquid surface. This phase is designated as the source and is the less dense of the two. Receptor and the source solutions are mutually insoluble. As the diffusion proceeded, changes of phenol concentrations in the receptor were monitored by absorbance measurements with time at different temperatures. The same procedure was followed for experiments in which phenol+CTAB aqueous solutions (source) were placed on the top of pure tetrachloroethylene (receptor). In this case, the initial concentration of phenol in the source phase was 1 wt%.

Results and discussion

Rheometry

The rheological measurements were carried out on the aqueous micellar solution of CTAB in the presence of phenol. The concentration of CTAB in water was kept fixed at 0.15 M (5.5 wt%) and 0.1 M (3.6 wt%), varying the phenol concentration expressed in weight percent in the total system. Figure 1 shows the representative plot at 30 °C for steady shear rate $\left(\dot{\gamma}\right)$ vs viscosity (η) curves for 0.15 M CTAB solution with increasing phenol concentration. At lower phenol content (up to 0.5 wt%) in the system, the solution shows Newtonian behavior over the entire range of shear rate studied. With the further increase in phenol concentration, the viscosity increases sharply and non-Newtonian, shear-thinning behavior is observed at higher$\dot{\gamma}$. This behavior is typical of worm-like micelles solutions in which the viscosity decreases above certain critical $\dot{\gamma}$ due to shear alignment of the micelles and breaking of the structured networks. With the increase in phenol concentration, the worm-like micelles become more structured and the critical $\dot{\gamma}$ shifts to lower values, and when the phenol concentration is 1.5 w%, the sample becomes highly viscoelastic and attains a maximum value of viscosity

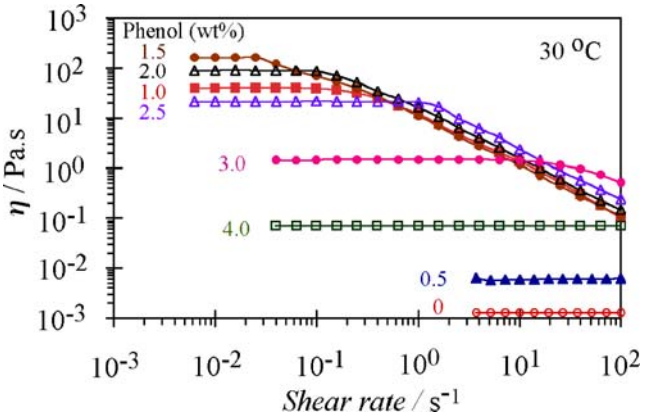

Fig. 1 Steady shear-rate plots for 0.15 M CTAB aqueous solutions as a function of phenol concentration at 30 °C. *Lines* are only visual guides

(~165 Pa.s). With further increase in phenol concentration, the viscosity decreases, which corresponds to a structural change in the system as indicated by a drop in the magnitude of the Newtonian plateau in the η vs $\dot{\gamma}$ curve [31].

Figure 2 shows the variation of zero-shear viscosity (η_0) for different CTAB concentrations in water in the presence of phenol at 30 °C. The values of η_0 were obtained from steady-shear rheological experiments in the limit of low shear rates, where the viscosity approached a plateau. Upon addition of phenol, viscosity shows a tremendous increase (almost six orders of magnitude) until a maximum is reached and then decreases. However, the magnitude of the viscosity is much larger at a CTAB concentration of 0.15 M as compared to 0.1 M, which is attributed to the decrease in the interfacial cross-sectional area, a_s, of surfactant at the interface with increasing surfactant concentration. The gel-like samples are isotropic at rest but shows shear birefringence, which is typical for solutions containing worm-like micelles. It is well known that there is a transition from linear to branched micelles at the peak [32], namely, micelles grow in one dimension before reaching the peak composition and thereafter tend to form branches that induce a drop in viscosity because the branching points are not fixed but are free to slide along the micelle providing an additional mode of stress relaxation [32].

Temperature dependence of the rheological spectra were measured to understand the effect of temperature and hence to get an insight into the flexibility of the micelles. As seen in Fig. 3, the behavior is typical (at least qualitatively) of ionic surfactant systems, namely, when a worm-like micellar solution is heated, the micellar contour length L decays with temperature according to [3, 31],

$$L = \phi^{1/2} \exp\left[\frac{E_c}{2k_B T}\right] \quad (1)$$

Where ϕ is the volume fraction of worms, E_c is the end-cap energy (i.e., the excess energy associated with the hemispherical caps compared to the cylindrical body of the worm), and k_B is Boltzmann's constant. This behavior is attributed to the fact that, at higher temperatures, surfactant unimers can hop more rapidly between the cylindrical body and the hemispherical end-caps of the worm. The reduction in micellar length, in turn, leads to a decrease in viscosity. The effect of temperature can be visualized clearly on the zero-shear viscosity plot for the 0.15 M CTAB in the presence of phenol at 30 and 35 °C (Fig. 3). The η_0 decreases considerably with an increase in the temperature from 30 to 35 °C.

To characterize the viscoelasticity of water/CTAB/phenol system, we turned to dynamic rheology. Oscillatory-shear (frequency sweep) measurements were performed on the viscoelastic samples formed around the viscosity maximum. Figure 4 shows representative dynamic plots for the 0.15 M CTAB in the presence of 2.5 wt% phenol, depicting the variation of the elastic or storage modulus (G') and the viscous or loss modulus (G'') with oscillation frequency (ω)

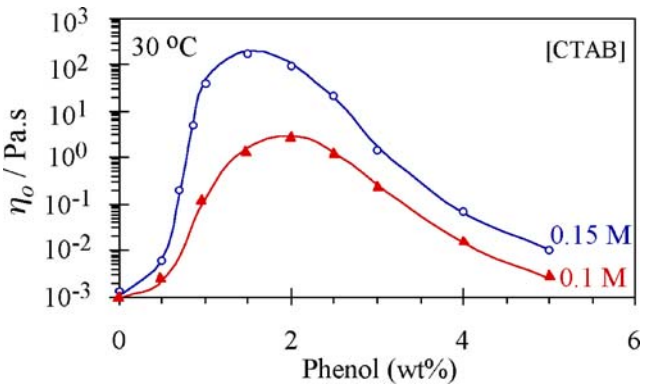

Fig. 2 Plots of the zero-shear viscosity (η_0) at different CTAB concentrations (0.1 and 0.15 M) in aqueous solution as a function of phenol concentration at 30 °C. *Lines* are only visual guides

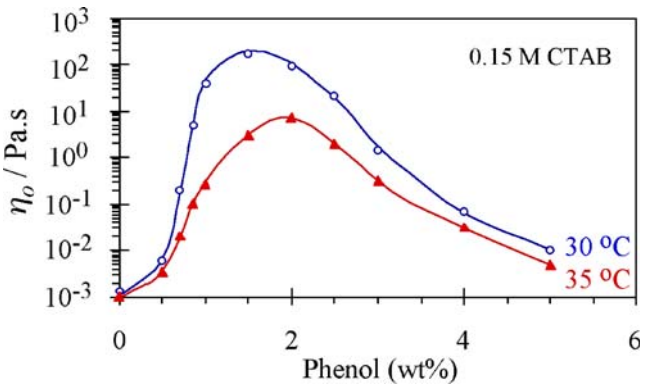

Fig. 3 Plots of the zero-shear viscosity (η_0) for 0.15 M CTAB aqueous solutions as a function of phenol concentration at different temperatures (30 and 35 °C). *Lines* are only visual guides

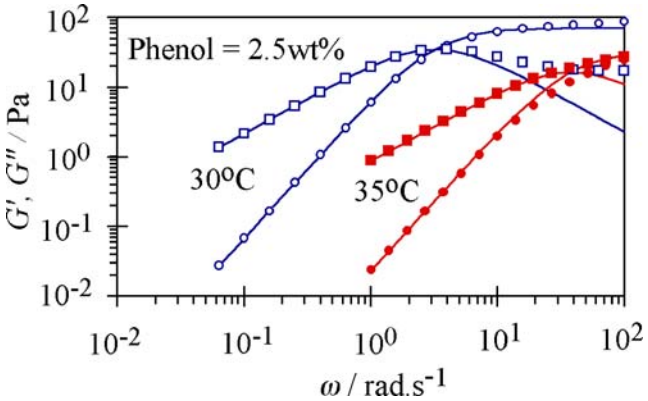

Fig. 4 The variation of the elastic or storage modulus G' (*circles*) and the viscous or loss modulus G'' (*squares*) with the oscillation frequency (ω) for the aqueous 0.15 M CTAB solution in the presence of 2.5 wt% phenol at 30 °C (open symbols) and 35 °C (closed symbols)

at 30 and 35 °C. The data clearly reveal the viscoelastic response of these samples. It shows a liquid-like behavior ($G'<G''$) at the low frequency and solid-like behavior ($G'>G''$) at the high frequency. In the low ω region, the data points could be fitted to the Maxwell equations, but in the high ω region, experimental data deviate from the model, which is generally attributed to faster relaxation processes such as Rouse modes. Maxwellian type oscillatory rheological behavior of viscous micellar solutions can be related to the transient network formed by the entanglement of worm-like micelles [3].

In the Maxwell model of viscoelastic fluids with a single relaxation time (τ_R), G' and G'' obey the following relations as a function of ω *[33].*

$$G'(\omega) = \frac{(\omega\tau_R)^2}{1+(\omega\tau_R)^2} G_0 \qquad (2)$$

$$G''(\omega) = \frac{\omega\tau_R}{1+(\omega\tau_R)^2} G_0 \qquad (3)$$

The plateau modulus, G_o, is given by G' (ω) at high ω. The relaxation time, τ_R, may be estimated from the relation, $\tau_R=1/\omega_c$, where ω_c is the G'–G'' cross-over frequency. Using G_o and τ_R, η_0 can be calculated using following relation [33]

$$\eta_0 = G_o\tau_R \qquad (4)$$

The results in Fig. 4 show that with increasing temperature, the entire frequency spectrum shifts to higher frequencies (i.e., shorter time scales), which suggests faster relaxation processes attributed to the decrease in micellar length.

Figure 5 shows the variation of dynamic rheological parameters G_o and τ_R for the aqueous 0.15 M CTAB system as a function of phenol concentration, obtained from the Maxwellian fit to the experimental data at 30 and 35 °C. As the values of G_o are related to the number of entanglements between worm-like micelles or the mesh size of the network, the increase in G_o with the phenol concentration corresponds to the increase in the network density of the worm-like aggregates. On the other hand, τ_R at first increases along with the increasing G_o as the concentration of phenol increases, which may be associated with the increase in the micellar contour length attributed to an increase in the curvature energy of the surfactant molecules in the end-cap. After saturation of the micellar growth, further addition of phenol results in the connection of the worm-like micelles with each other, forming a joint that can slip along its length. The relaxation time τ_R is determined by a competition between micellar breaking and chain reptation; Maxwellian behavior is generally observed when the breaking time τ_B is much lower than the reptation time τ_{rep}. In this fast breaking regime, the relaxation time $\tau_R \sim (\tau_B\tau_{rep})^{1/2}$. The magnitude of both G_o and τ_R decrease with an increase in temperature, reflecting less dense networks and faster relaxation.

Spectrometry

Mass transfer of phenol from an organic phase to an aqueous phase

All the measurements were performed as described in the experimental section to study the diffusion of phenol from octanol to pure water or aqueous surfactant solutions. As depicted in Fig. 6a, phenol in CTAB showed a clear absorbance band at around 275 nm and a shoulder near 280 nm, in agreement with previous reports [34, 35], which was used to monitor concentrations. The absorbance as a function of time was measured in the contacting experiments.

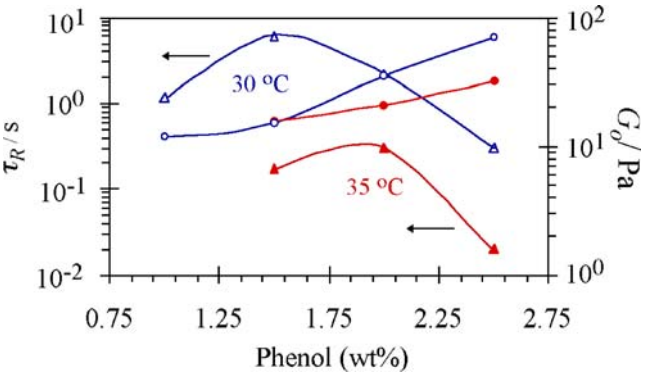

Fig. 5 The variation of plateau modulus G_o (*circles*) and relaxation time τ_R (*triangles*) in aqueous 0.15 M CTAB solution as a function of phenol concentration at 30 °C (*open symbols*) and 35 °C (*closed symbols*)

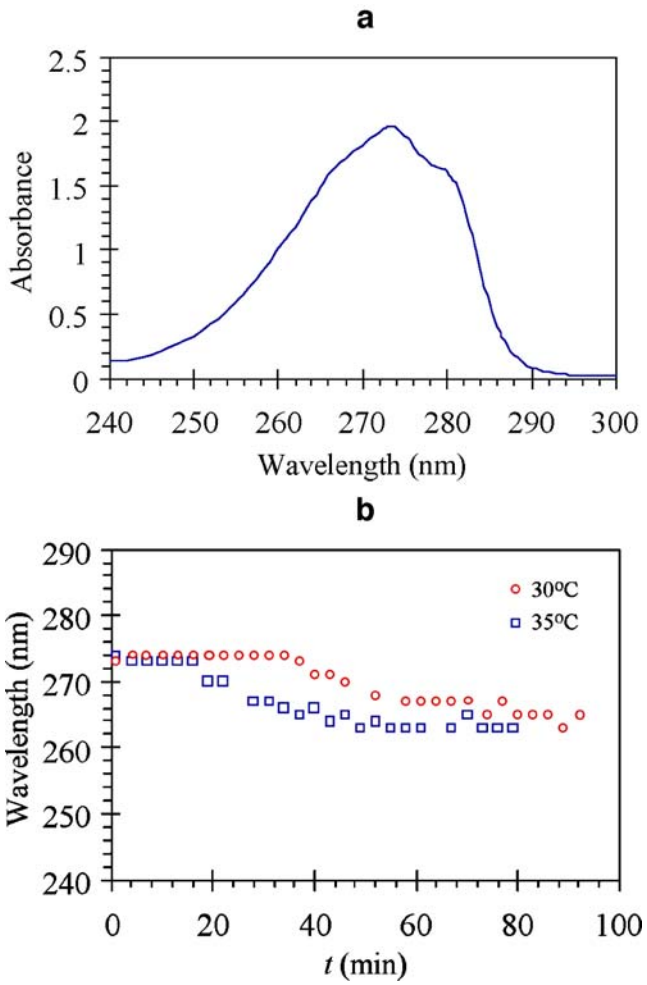

Fig. 6 **a** Representative UV spectra of phenol in 0.15 M CTAB aqueous solutions at 30 °C. **b** Change of the maximum of the phenol absorption band with time for aqueous 0.15 M CTAB solution as receptor and octanol as the source at two different temperatures (30 and 35 °C)

Initially (i.e., just after placing the cuvette in the spectrometer), there is no detectable band in the 240- to 300-nm wavelength range, but after a short time, a band around 275 nm appears, which is attributed to the diffusion of phenol. The increase in the band intensity is associated to an increase in the phenol concentration; however, the rate of change is higher in the case of water (faster diffusion of phenol) as compared to the 0.15 M CTAB solution. As shown in Fig. 6b, the band position suffers a blue (hypsochromic) shift with time from around 275 nm to about 262 nm, which is probably related to the change in phenol hydration or surrounding microenvironment as phenol interacts with CTAB. This change seems to be faster as temperature is increased. Longer absorption wavelengths would be expected for phenol in a non-polar environment; in fact, red (bathochromic) shifts are observed when hydrophobic probes are solubilized inside micellar aggregates. Therefore, in the present case, phenol apparently is not solubilized in the non-polar interior of CTAB micelles but rather stays at the interface forming hydrogen bonds, in agreement with previous reports [35]. Such an interaction would favor changes in the surface area of aggregates, which promotes the micellar growth detected by rheometry.

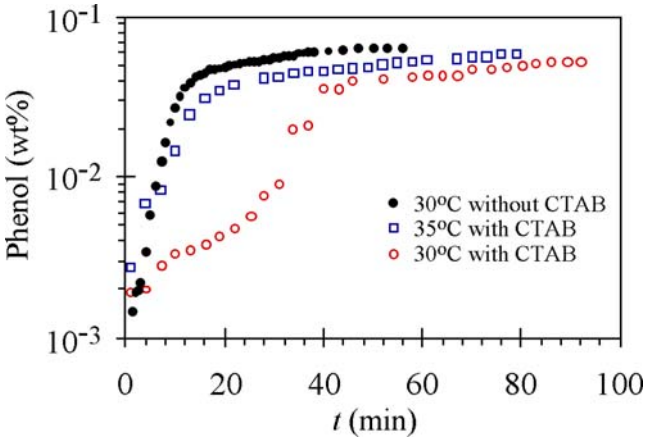

Fig. 7 Change of phenol concentration with time in the aqueous 0.15 M CTAB solution (receptor) having octanol as source at different temperatures (30 and 35 °C). Data for pure water as receptor is also included for comparison

We can get a clear idea about the diffusion of phenol from Fig. 7. The change in phenol concentration in the receptor is slower in the presence of CTAB, especially at short times, namely, the surfactant hinders the diffusion of phenol. However, when temperature is increased, the transfer of phenol is significantly accelerated. The maximum attained concentration in the receptor solution is also lower in the presence of CTAB due to a different partition of phenol when micelles are present. There are several

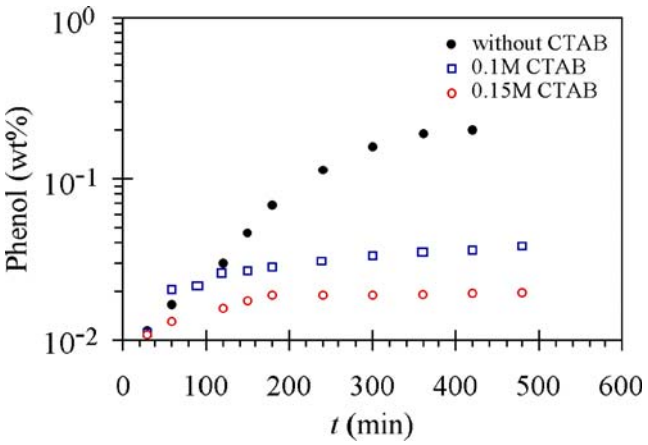

Fig. 8 Change of phenol concentration with time in tetrachloroethylene (receptor) having CTAB solutions as sources at two different concentrations, 0.15 M CTAB (*open circles*) and 0.1 M CTAB (*squares*). Data for pure water as source (*filled circles*) are also included for comparison. The initial concentration of phenol in the source phase was 1 wt%

limitations in trying to derive the values of diffusion coefficients from the contacting experiments used in the present study [35]; moreover, the resolution of mass transfer equations is quite complex, as in the present system, a viscoelastic network might be formed as the solute diffuses. Hence, we focused on a qualitative interpretation of the results. It is known that the presence of micelles leads to a decrease in the apparent diffusion coefficient [36] due to association, solubilization, or binding.

Above the critical micellar concentration (cmc), the solute molecules in the bulk phase diffuse with a diffusion coefficient D_w, while solutes in the micellar pseudophase diffuse with the diffusion coefficient of the micelle (D_m), which is much lower than D_w. Thus, the diffusion coefficient is the average of the solute diffusion in the two phases. It is evident that D_m will be significantly lower if the micelles are large and entangled forming viscoelastic networks. The phenol concentrations plotted in Fig. 7 are the average seen by the spectrophotometer over a certain distance within the cuvette; however, along such a distance, there is a concentration gradient. Considering the concentration range of the data in Fig. 7, at first glance, it seems that the systems are below the viscoelastic regime detected from Fig. 2. However, as there is a concentration gradient, the local concentrations near the interface would be much higher than the values depicted in Fig. 7. Namely, it is possible that worm-micellar solutions are present near the interface, which would significantly increase the resistance to mass transfer. When there is interface resistance, the concentrations in either side of the interface are no longer constant, but each approaches the equilibrium value relatively slowly [37]. This would explain the significant retardation of phenol diffusion observed at short times and at 30 °C in Fig. 7. An increase in temperature causes the disruption of long micelles, and therefore, the mass transfer is accelerated.

Mass transfer of phenol from an aqueous phase to an organic phase

The diffusion of phenol from water or aqueous CTAB solutions (source) to tetrachloroethylene (receptor) was also studied, and the results are plotted in Fig. 8. Again, there is a significant decrease in the velocity of mass transfer in the presence of CTAB, which is proportional to CTAB concentration. However and contrary to Fig. 7, the phenol concentrations in the receptor remain low in the investigated time frame when CTAB is added to the source solution, reflecting changes in the partition coefficients.

The initial source CTAB+phenol aqueous solutions used in the contacting experiments depicted in Fig. 8 are already in the viscoelastic region (see Fig. 2), which explains the significant retardation of phenol transfer towards the organic phase, due to the slow diffusion of the long, entangled micelles to which phenol molecules are strongly associated. It is worth mentioning again that the viscoelastic nature of the solution weakens with the decrease in CTAB concentration. The decrease in viscosity with the decrease in CTAB concentration (Fig. 2) agrees well with the observed acceleration of phenol transfer towards the organic phase.

Conclusions

The cationic surfactant hexadecyltrimethylammonium bromide (CTAB) self assemble into giant worm-like micelles in the presence of the phenol, giving rise to unusually strong viscoelasticity. The presence of phenol with negative polarity favors the screening of repulsive interactions between the positively charged head groups of CTAB, leading to a decrease in the specific surface area, which in turns promotes the formation of worm-like structures. The presence of large CTAB micelles hinders the diffusion of phenol, but this hindrance decreases with an increase in temperature. The above study offers the potential of regulating the mass transfer, which may be exploited in applications.

Acknowledgement DV thanks Japan Society for Promotion of Science (JSPS) for financial support. This work was supported by The Ministry of Education, Culture, Sports, Science, and Technology, Grant-in-Aid for Young Scientists (B), No. 18780094 and partly supported by Core Research for Evolution Science and Technology (CREST) of JST Corporation.

References

1. Walker LM (2001) Curr Opin Colloid Interface Sci 6:451
2. Yang J (2002) Curr Opin Colloid Interface Sci 7:276
3. Cates ME, Candau SJ (1990) J Phys Condens Matter 2:6869
4. Rehage H, Hoffmann H (1988) J Phys Chem 92:4712
5. Kern F, Lemarechal P, Candau SJ, Cates ME (1992) Langmuir 8:437
6. Hassan PA, Candau SJ, Kern F, Manohar C (1998) Langmuir 14:6025
7. Shikata T, Shiokawa M, Imai S (2003) J Colloid Interface Sci 259:367
8. Raghavan SR, Fritz G, Kaler EW (2002) Langmuir 18:3797
9. Kim W-J, Yang S-M (2000) J Colloid Interface Sci 232:225–234
10. Rodriguez C, Acharya DP, Maestro A, Hattori K, Kunieda H (2004) J Chem Eng Jpn 37:622
11. Acharya DP, Hattori K, Sakai T, Kunieda H (2003) Langmuir 19:9173
12. Engelskirchen S, Acharya DP, Garcia-Roman M, Kunieda H (2006) Colloids Surf A 279:113

13. Hoffmann H (1994) In: Herb CA, Prudhomme R (eds) Structures and flow in surfactant solutions; ACS Symposium Series 578. American Chemical Society, Washington, DC, p 2031
14. Toernblom M, Henriksson U (1997) J Phys Chem B 101:6028
15. Nagarajan R (1996) Curr Opin Colloid Interface Sci 1:391
16. Hedin N, Sitnikov R, Furo I, Henriksson U, Regev O (1999) J Phys Chem B 103:9631
17. Rodriguez C, Aramaki K, Tanaka Y, Arturo Lopez-Quintela M, Ishitobi M, Kunieda H (2005) J Colloid Interface Sci 291:560
18. Sato T, Acharya DP, Kaneko M, Aramaki K, Singh Y, Ishitobi M, Kunieda H (2006) J Dispersion Sci Techn 27:611
19. Stradner A, Glatter O, Schurtenberger P (2000) Langmuir 16:5354
20. Zhang WC, Li GZ, Shen Q, Mu JH (2000) Colloids Surf A 170:59
21. Penfold J, Staples E, Tucker I (2002) J Phys Chem B 106:8891
22. Dunn Jr RO, Scamehorn JF, Christian SD (1985) Sep Sci Technol 20:257
23. Akkara JA, Ayyagari M, Bruno F, Samuelson L, John VT, Karayigitoglu C, Tripathy S, Marx KA, Rao DVGLN, Kaplan DL (1994) Biomimetics 2:331
24. Premchandran R, Banerjee S, John VT, McPherson GL, Akkara JA, Kaplan DL, Ayyagari M (1996) Macromolecules 29:6452
25. Liu W, Kumar J, Tripathy S, Samuelson L (2002) Langmuir 18:25
26. Bunt o n CA, Cowell CP (1988) J Colloid Interface Sci 122:154
27. Busserolles K, Roux-Desgranges G, Roux AH (1997) Progr Colloid Polym Sci 105:326
28. Mata JP, Aswal VK, Hassan PA, Bahadur P (2006) J Colloid Interface Sci 299:910
29. Agarwal V, Singh M, McPherson G, John V, Bose A (2006) Colloids Surf A 281:246
30. Williams CL, Bhakta AR, Neogi P (1999) J Phys Chem B 103:3242
31. Raghavan SR, Kaler EW (2001) Langmuir 17:300
32. Lequeux F (1992) Europhys Lett 19:675
33. Larsen RG (1999) The structure and rheology of complex fluids. Oxford University Press, Oxford
34. Tchaikovskaya ON, Mikhaleva IA (2004) Russ Phys J 47:11
35. Nemethy G, Ray A (1973) J Phys Chem 77:64
36. Yang X-N, Matthews MA (2000) J Colloid Interface Sci 229:53
37. Crank J (1989) The mathematics of diffusion. Oxford University Press, New York